INSTITUTE OF PLASMA PHYSICS

NAGOYA UNIVERSITY

Modern Uses of Langmuir Probes

Francis F. Chen

(Received – Sept. 26, 1985)

IPPJ- 750 Nov. 1985

RESEARCH REPORT

NAGOYA, JAPAN

Modern Uses of Langmuir Probes

Francis F.Chen*

(Received - Sep. 26, 1985)

IPPJ-750 Nov. 1985

Notes from lectures given at Nagoya April 25; at Hefei, China, May 21; and at Beijing, China, May 27, 1985.

*Permanent address: Electrical Engineering Department, University of California, Los Angeles, CA 90024

Modern Uses of Langmuir Probes

Francis F. Chen*

ABSTRACT

The Langmuir probe is adaptable to measurements in strong rf and strong magnetic fields such as exist in many fusion related experiments. Some new techniques, mostly untested, are described which could be developed to overcome the difficulties of this diagnoshtic method.

I. INTRODUCTION

In plasmas in which a Langmuir probe can survive, this diagnostic remains the easiest and most accurate way to make local measurements. Such plasmas are, for instance, the edge regions of a tokamak and all toruses, mirrors, and alternate fusion configurations in which the density is below 10^{12} cm^{-3} . It is particularly important to avoid runaway electrons and other energetic species which can melt the probe. However, new probe techniques must be developed to make measurements in strong magnetic fields and strong rf fields, such as exist in many small-scale experiments concerning the physics of rf heating, current drive, and confinement. In this paper we first review the principal ideas in probe techniques and then suggest some new ideas which can extend the usefulness of probes in present-day plasmas.

II. BRIEF REVIEW

1. Probe characteristic. The notation for a standard I-V characteristic is shown in Fig.1. I is the electron current into the probe, V the probe voltage relative to ground, I_i the ion saturation current, I_e the electron saturation current, and V_f the floating potential. The probe will be assumed to be a cylinder of radius a and length L. The collecting area for ions with $r_L \gg a$ is $A_i = 2\pi a L$, and that for electrons with $r_L \ll a$ is $A_e = 4aL$. However, since the sheath fields will be distorted by $\underline{B}$, it will be sufficiently accurate to take $A = 4aL$ for both species.

2. Presheath. for $V < V_f$, most electrons are repelled by the sheath, and f_e (v) can be approximated by a Maxwellian. However, the ions at the sheath edge must be unidirectional, and hence there must be a weak accelerating field in a large "presheath" between the field-free plasma and the sheath edge. The presheath field accelerates the ions so that they enter the sheath with a directed velocity V_B, the Bohm velocity, which for $T_e \gg T_i$ is given approximately by

$$V_B = 0.5(KT_e/M)^{1/2}. \tag{1}$$

Thus, the ion saturation current is

$$I_i = 0.5neA(KT_e/M)^{1/2}. \tag{2}$$

3. Output impedance. At $V=V_f$, I changes by $\simeq I_i$ for a change in V of order KT_e/e. Thus, the effective output impedance R_o at V_f is

$$R_o = T_{eV}/I_i$$

For example, if a = 0.25mm, L=2mm, T_{eV} = 10, n = 10^{11} cm^{-3}, and M = $4M_H$, then A = 0.02 cm^2 and

$$V_B = (0.5)[(10)(1.6\times10^{-12})/(4)(1.67\times10^{-24})]^{1/2} = 7.7\times10^5 cm/sec$$

$$I_i = (10^{11})(2\times10^{-2})(7.7\times10^5)(1.6\times10^{-19}) = 0.25mA,$$

and

$$R_o = 10/2.5\times10^{-4} = 40k\Omega$$

4. Load line. When the probe is connected to a measuring resistor R, the operating point is the intersection between the probe characteristic and a load line of negative slope R (due to the fact that I is defined as an electron current), as shown in Fig.2. For current measurements (Fig.3), R has to be small so that the operating point gives I correctly regardless of the applied voltage V. For potential measurements (Fig.4), R has to be large, so that the operating point lies close to V_f. As a rough guide, one can take $R \ll R_o$ for I measurements and $R \gg R_o$ for V_f measurements. However, if large rf potentials $\tilde{V}_{rf}$ exist in the plasma, the I-V curve may be displaced very far from ground, and the condition on R is more severe. In Fig.5, we see that R_2 would give a false reading of V_f, and a larger resistance R_1 is necessary. Since V can be $\gtrsim \tilde{V}_{rf}$ and we want $|I| \ll I_i$, the condition on R for potential measurements is

$$R \gg V_{rf}/I_i,$$

which can be $\gg R_0$. On the other hand, measurements of I_i require only that

$$R \ll R_o(I_i),$$

where $R_o(I_i) \gg R_o(V_f)$, since the slope of the I-V curve in the I_i region is very small. Thus, in the presence of large rf fields, it is much easier to measure I accurately than to measure V_f.

5. Frequency response. In measuring fluctuations in V_f, the frequency response of the circuit is limited by the stray capacitance C, which is mainly the capacitance of the cable connecting the probe to the amplifier. Since $R \gg R_0$, the time constant is R_0C. For instance, if $R_0 = 40k\Omega$ and C=300pF due to 3 meters of cable with 1 pF/cm, $1/R_0C$ is 83 kHz. This example was for $n=10^{11}$ cm^{-3}, and the frequency response would be 10 times better at 10^{12} cm^{-3}. Nonetheless, it is clear that a floating probe cannot follow rf frquencies of order 10MHz accurately without special precautions. One possibility is to place a transistor stage inside the probe shaft, thus lowering C to a few picofarads. This method, however, is limited by the ability of solid state devices to operate in strong magnetic fields.

6. Capacitance neutralization. In Fig.6, we show the standard method [1] for improving frequency response by capacitance neutralization. A doubly shielded probe is used, and a unity-gain amplifier is connected across the stray capacitance C. Since the potential across C is reduced to nearly zero, no current flows through C, and the loss of high frequencies does not occur. Typically, if the gain is 0.999, C is effectively reduced by 10^3 and the frequency response improved by a factor 10^3. The limit is now the frequency response of the amplifier, which must be rolled off to prevent high-frequency oscillation. The amplifier must have low enough output impedance to drive the capacitance C_1 between the inner shield and ground.

7. Double probes. When the plasma potential fluctuates greatly, it is common practice to use floating double probes, which can follow the fluctuations and avoid a) nonlinear probe response and b) overheating by excessive electron current. Fig.7 shows a typical circuit and a schematic I-V curve. The probe current is limited by the ion saturation current to one probe or the other, and the slope at V=0 in principle yields T_e. Such a probe can be used in pulsed plasmas up to densities of 10^{16}-$10^{17} cm^{-3}$ if the resistor R is replaced by a current transformer and the power supply is replaced by a capacitor bank to supply the large probe currents. However, the occurrence of unipolar arcs to the probe tips limits the usefulness of this diagnostic at such high densities[2].

We do not recommend the use of double probes for several reasons. First, the system cannot truly float ac-wise because of the large stray capacitance C between the power supply and ground. This supply is usually quite difficult to shield by capacitance neutralization. Second, the temperature measurement concerns only the fast electrons in the tail of the distribution, not those in the body of the distribution. Third, the positioning of the probes in a strong magnetic field is rather tricky. If the two probe tips lie on the same tube of force, the probes are in each other's shadow. If the probe tips are on different tubes of force, they may be sampling different plasma potentials. Thus, the tips must be rotated so that they lie on adjacent tubes of force and just out of each other's shadow, as shown in Fig.8.

8. Hot probes. An emitting probe is often used to measure the plasma potential V_s, as contrasted with the floating potential V_f. An additional advantage is that the output impedance R_0 is reduced. Fig.9 shows an idealized I-V curve for a hot probe. When $V > V_s$, the emitted electrons cannot leave the probe, and the probe collects the saturation electron current I_e. When $V<V_s$, the thermionically emitted current I_t leaves; and if $I_t > I_e$, the net current reverses. Thus, the I-V curve is nearly vertical, and V_f lies close to V_s. The ion current is negligible in this case.

There are two ways to construct a hot probe, both of which have been used successfully. In Fig.11, the probe is a thin tungsten wire loop heated by current from a transformer. To avoid magnetic field effects due to the heating current, readings are made only during the current null. This method has three drawbacks: the wire breaks easily, the transformer has large stray capacitance to ground, and the emitting area is not well defined. In Fig.12, the probe is a small sphere heated by ion bombardment. The large negative heating voltage V_0 is switched on and off by a large SCR (silicon controlled rectifier) or similar device. In the off state, the heating circuit is effectively removed from the measuring circuit, and the probe remains hot for several milliseconds, during which readings can be made. The ion sheath will return to normal in a time of order Ω_{pi}^{-1}.

Hot probes, however, do not always operate under the ideal conditions giving the I-V curve of Fig.9. Since the emitted electrons have temperatures of order $KT_c \simeq 0.2$ eV, there is usually an asymmetry caused by $T_e \gg T_c$. The slow electrons cannot leave the probe fast enough and form a space charge layer close to the probe surface. The

resultant double sheath, shown in Fig.10, repels the emitted electrons, forcing the emitted current to obey a space charge limit. Since the extra negative dip is scaled to T_c, which is small, the probe then floats close to V_f, rather than V_s, Thus, it is not assured that a hot probe will always float at $V=V_s$.

9. Plasma potential in strong magnetic fields. Before discussing measurements of plasma potential, one has to clarify what is meant by plasma potential, because this concept is not simple in a strong magnetic field. As soon as a probe with a $\gg r_{Le}$ is inserted in to a plasma, the entire flux tube intersecting the probe is disturbed, as shown in Fig.13, because the flux of electrons to each region within the flux tube is disrupted by the probe. Thus, the potential at the probe position is not the same as the space potential that was there before the probe was inserted. The situation is even worse for large objects such as gridded velocity analyzers or magnetic probes. If the probe is biased to draw electron current, the depletion of density in the disturbed flux tube limits I_e to $\simeq 10 I_i$ rather than $\simeq (M/m)^{1/2} I_i$, as in the B=0 case. The voltage at the "knee" of the curve (Fig.1) in the case of strong B no longer bears a simple relation to V_s. If the probe is biased to draw ions or is floating, it will reflect most of the electrons, and the disturbance is minimized. Presheath acceleration of ions is still necessary, so the potential inside the perturbed flux tube must be negative, as shown in Fig.13. The density there must also be lower than outside, by approximately a factor of 2 (essentially the factor 0.5 of eq.(2)). The electron population in the disturbed flux

tube is replenished by electron diffusion. If the horizontal scale is contracted by a factor $\simeq D_{\parallel}/D_{\perp}$, the disturbed region is like the ellipsoid shown in Fig.14. The space potential V_s is the potential outside of this region, but in open-ended machines the endplate may be located inside the region, in which case V_s may not be related to V_f. Electrons diffuse into the perturbed region <u>against</u> the electric field. In most plasmas electrons have an anomalously large $D_{\perp}$ due to high-frequency fluctuations. It is this effect that reduces the length of the perturbed region and enables one to use probes in a strong B-field.

10. <u>Measurements of V_s in a B-field</u>. The best way to measure V_s is to measure V_f with a cold or hot probe, and then to correct for the difference. Let V_s' be the potential at the sheath edge. Inside the perturbed flux tube, the balance of ion and electron currents to a cold probe requires

$$nV_B = nV_e \exp\ [-e(V_s'-V_f)/KT_e\ ]$$

where $V_B = 0.5(KT_e/M)^{1/2}$ and $V_e = (KT_e/2\pi m)^{1/2}$. Since the presheath potential is $\simeq KT_e/2e$, we have $V_s = V_s'+KT_e/2_e$ and

$$V_s = V_f + \frac{1}{2}\frac{KT_e}{e} + \frac{KT_e}{e} ln(\frac{2M}{\pi m})^{1/2}, \qquad (3)$$

This must be quite rigorously obeyed; therefore, it is better to measure V_f rather than V_s directly by drawing large electron currents. For a hot probe, the correction term is smaller, but it is more uncertain because of double-sheath effects. Since heat conductivity is high in

modern-day plasmas, it is unlikely that KT_e will fluctuate. Then fluctuations $\tilde{V}_s$ can be measured directly by observing $\tilde{V}_f$. The only other condition on the use of Eq. (3) is that the electron $D_\perp$ must be large enough that the disturbed flux tube does not run into a wall.

III. USE OF PROBES IN STRONG RF FIELDS

1. Electromagnetic pickup. Fig.15 illustrates the problem of electromagnetic pickup. Current in the antenna structure will cause oscillating fields $\tilde{B}$ in the plasma and vacuum. If the probe circuit encloses any of this $\tilde{B}$, an undesired inductive signal will be picked up through the capacitance of the probe sheath. The size of this signal depends on the size of the pickup loop. If the ground return to the probe occurs through the probe shaft, then across the plasma to the probe tip (path 1), then the loop is small. If the ground return goes from the vacuum chamber through the highly conducting plasma (path 2), the loop will be large. There may be other paths, and all of them can be active simultaneously. The pickup signal also depends on the rf field pattern, the electron parallel conductivity, and the ion transverse conductivity. Thus it is impossible to calculate the pickup and correct for it. However, one can check that the pickup is small and then neglect it. Such a check can be made, for instance, by covering the probe with a glass sleeve and correcting for the difference in capacitance between the sleeve and the probe sheath. Or one can apply different negative biases to the probe to vary the sheath thikness; the pickup should be more sensitive to this than the ion current

fluctuations.

2. Measurement of the probe characteristic. If the plasma potential oscillates with an amplitude V_{rf} , the probe characteristic will shift back and forth along the V axis, as shown in Fig.16. Because the I-V curve is nonlinear, the average current at an average voltage V will not be the same as the instantaneous current at voltage V. To remove the nonlinearity, one can use a two-probe method.[1] The two probes are mounted on the same shaft, as in a double probe, but they are connected independently. One probe is connected to a large resistor R_2 and measures instantaneous V_f . The other probe is connected to a small resistor R_1 and measures I. The signals at X and Y are connected to the X and Y axes of an oscilloscope. For any given setting of the bias voltage V, X gives the voltage relative to V_f as V_f fluctuates. Y gives the instantaneous current, which is fluctuating because V_s is fluctuating. The resulting scope trace is as in Fig.17 (B). As V is varied, the entire I-V curve is traced out, as in Fig.17(C), with the nonlinearity removed.

3. Measurement of dc space potential $\langle V_s \rangle$. The time-averaged potential is important in the study of thermal barriers and rf plugging in mirrors, but the presence of large ICRH fields makes this quantity difficult to measure. As explained above, it is sufficient to measure V_f and then correct it to obtain V_s . We propose a method to obtain $\overline{V_f}$ using a current measurement rather than a potential measurement, thus

avoiding the frequency response problem. As V_s oscillates with amplitude V_{rf} (Fig. 19), the probe characteristic will shift back and forth horizontally, so that the probe current is alternately positive and negative. If the probe is biased at $V=\overline{V}_f$, I will be positive half the time and negative half the time; otherwise, I will be positive or negative more than half the time. The magnitude of I is immaterial; only its sign matters. Fig.18 shows a circuit that will give $\overline{V}_f$. The probe is connected to measure I, and the I signal is fed to amplifier O_1, which is an opamp connected as a comparator. The input swings between I_e and I_i as V_s oscillates with amplitude $V_{rf} \gg KT_e/e$. The output of O_1 is a rectangular wave swinging between $+V_c$ and $-V_c$, where V_c is the power supply voltage. The average of this curve is in general nonzero. This signal is then applied to amplifier O_2, which is an opamp connected as an integrator with time comstant R_1C_1. The output of this is proportional to the asymmetry in the input signal. If the probe bias V is adjusted so that the output of O_2 is zero, then $V=\overline{V}_f$.

We propose a second, more complicated way to obtain $\overline{V}_f$. This is shown in Fig.20. The idea is to produce a trace like that in Fig.17(C), but without requiring a second probe, since the V_s oscillations are produced by an rf generator of known frequency and phase. (The scheme of Fig.17 will work even if V_S fluctuates randomly.) The probe is connected to measure current on the Y axis. The resistors R_1, R_2, R_3 form an adding network. The rf signals at W_o and its harmonics are derived from the rf generator, and each harmonic has an adjustable attenuator and phase-shifter. A signal simulating the V_s fluctuations is then synthesized and subtracted from the probe supply voltage to give the X signal. Before the synthesizer is turned on, the spot on the

oscilloscope display [*Fig.*17(*B*)] will be a vertical line. The probe voltage V is then adjusted so that the oscillations are around V_f. Then each harmonic is switched on in turn and adjusted in amplitude and phase to minimize the width of the display [*Fig.*17(*C*)]. If the I-V curve does not change during the rf cycle, this method will give the whole characteristic; otherwise, it will still yield $\overline{V}_f$ accurately.

4. Measurement of rf field distribution. The internal E-field created by an antenna is useful in studying the effectiveness of rf heating. Unfortunately, a single probe measures only V_f, and two derivatives of $V_f(\underline{r})$ have to be taken to get information on gradients in $\underline{E}$. To measure E directly, one can oscillate the probe between two positions, thus obtaining the difference in V_f directly. However, it is much simpler to move the plasma relative to the probe than the probe relative to the plasma. In Fig.21, we show how two coils producing a transverse magnetic field B_y can cause the plasma to be shifted by 1-2 mm in the y direction at a frequency W_m. In the absence of rf, the component of V_f signal from the probe which is phase-synchronous with the modulation at W_m (as detected by a lock-in amplifier) is directly proportional to the dc E_y. To measure E_x, one needs another set of coils producing B_x. This method has been used very successfully with dc fields[3]. When there are rf fields $\tilde{E}_{rf}$, the main probe signal will be at the rf frequency W_0. The amplitude of the sidebands at $W_0 \pm W_m$ will then be proportional to $\tilde{E}_{rf}$. The constant of proportionality can be obtained by measuring the plasma shift with an electron beam. To be sure the plasma moves adiabatically, the frequency W_m must be slow

compared with the ion acoustic transit time along $\underline{B_0}$; however, W_m must be high enough (>10Hz) to allow the use of synchronous detection.

To move the plasma by 1-2 mm requires very small fields $B_\perp$, and this measurement can be set up in two days. The supplementary coils can be wound by hand on a square wood frame, and they can be driven by an ordinary audio amplifier. Any rock group has enough power to provide the drive.

5. Measurement of low-frequency noise. The driven rf field inside a plasma can develop sidebands or be spread in frequency when there are low-frequency fluctuations in plasma potential. To detect these low-frequency fluctuations in the presence of a large rf signal, we propose to use V_{rf} as a probe sweep voltage. The probe is connected to measure current, as in Fig.18, and the I signal is again connected to a comparator. The output of amplifier O_1 will appear, in general, something like Fig.22(A). When V_{rf} is purely periodic, with no low-frequency noise, adjustment of the probe bias V can symmetrize the curve, as in Fig.22(B). Even if there is low-frequency noise, the condition $V=\bar{V}_f$ can be detected with an integrator, as in Fig.18. However, low-frequency noise will cause an irregularity in the zero-crossings of the wave in Fig.22(B), making it look like Fig.22(C), which has been exaggerated. Thus the low-frequency spectrum appears as a frequency modulation of the rf signal, which acts as a carrier. To recover the low-frequency spectrum, we can employ an ordinary FM receiver. First, the rf frequency must be converted to the if frequency of the receiver by heterodyning with an oscillator phase-locked to the

rf generator. Then the FM demodulator of the FM receiver can be allowed to work as usual. Since most low-frequency instabilities give frequencies below 100kHz, it is easy to obtain sufficient if bandwidth. However, one must be careful to remove the 19- and 38-kHz traps used for the stereo pilot signal and the muzak channel.

IV. ACKNOWLEDGMENT

The author thanks Profs. T.Uchida and Y.Ichikawa for their hospitality during a three-month visit to IPP, Nagoya.

REFERENCES

1. F.F.Chen, Proc. Int'l Conf. on Physics of Quiescent Plasmas, Frascati, Italy, Pt. II, 563 (1967).
2. J.J. Turechek and F.F.Chen, Phys. Fluids 24, 1126 (1981).
3. F.F.Chen and K.C.Rogers, Princeton PPL Report MATT-701 (1969, unpublished).

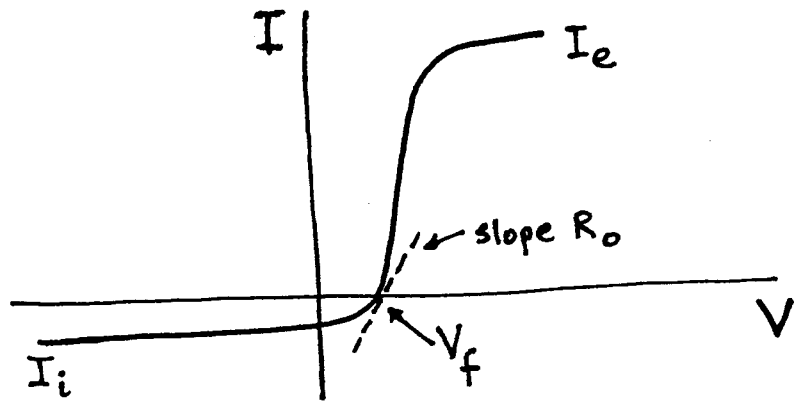

FIG. 1

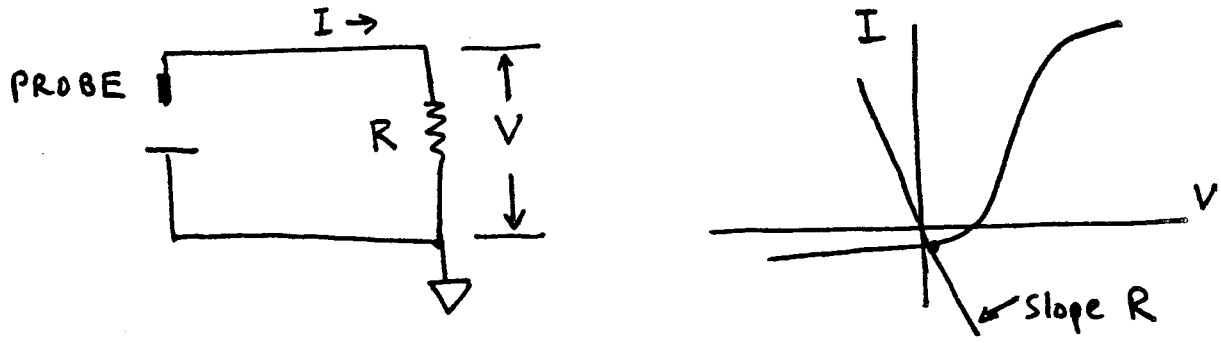

FIG. 2

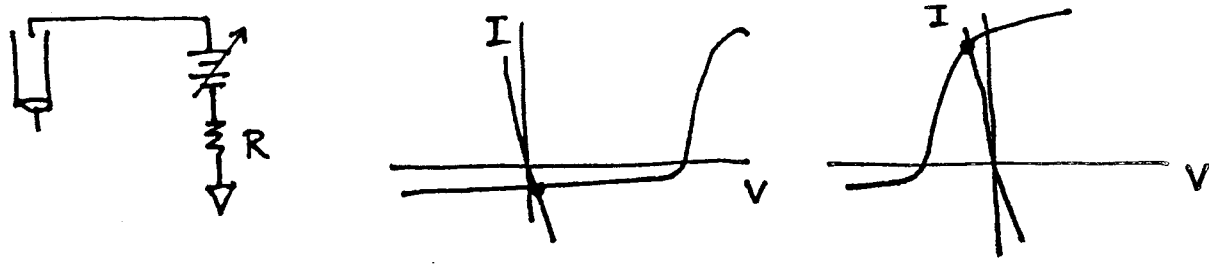

FIG. 3

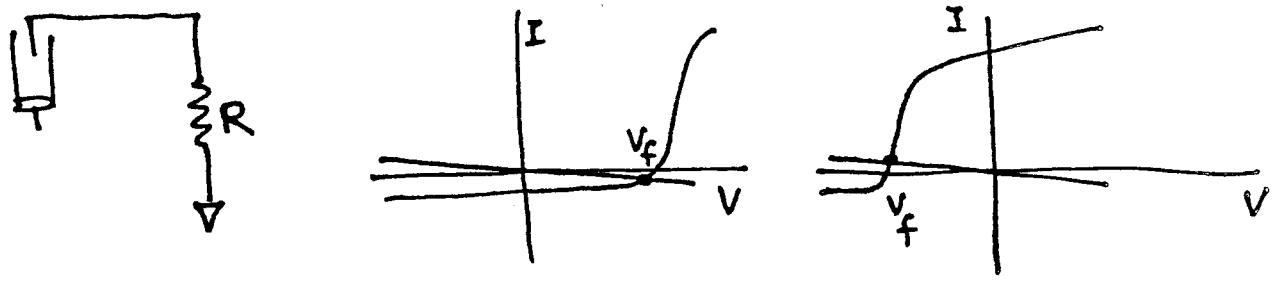

FIG. 4

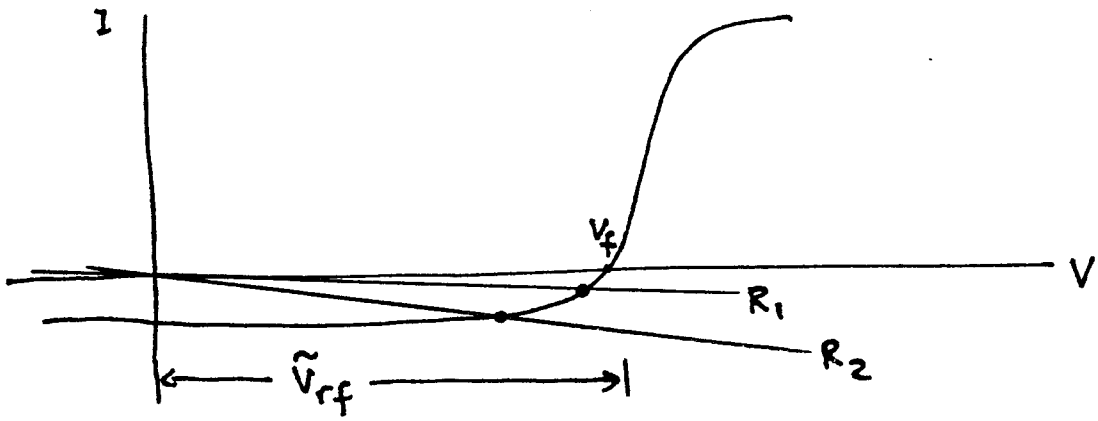

Fig. 5

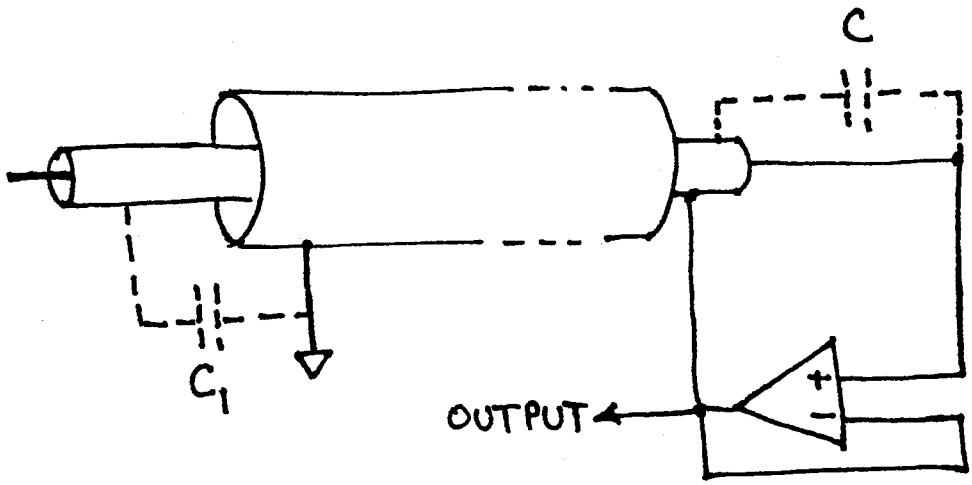

FIG. 6

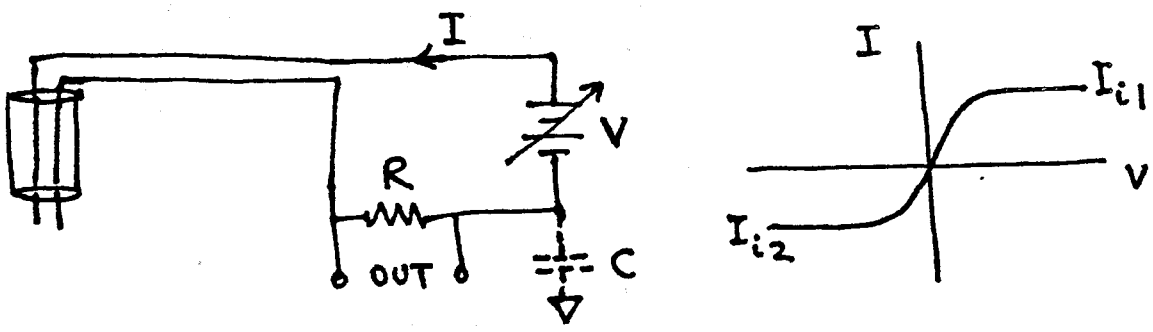

FIG. 7

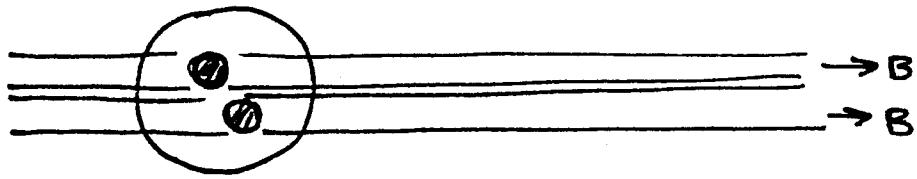

FIG. 8

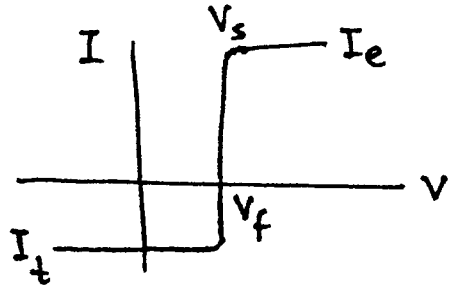

FIG. 9

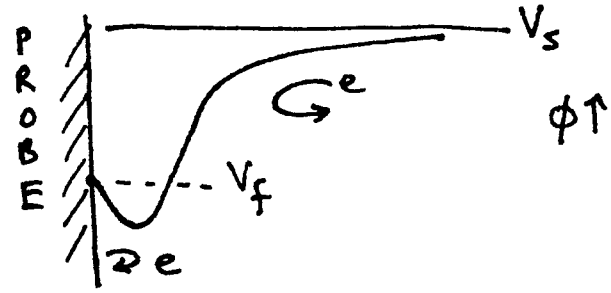

FIG. 10

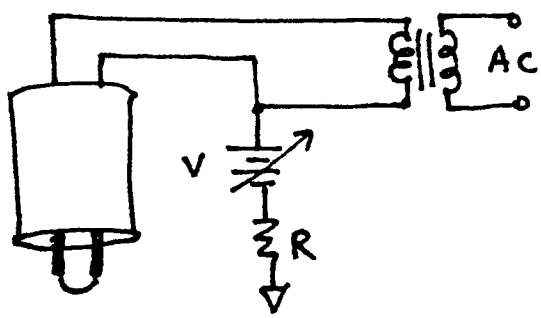

FIG. 11

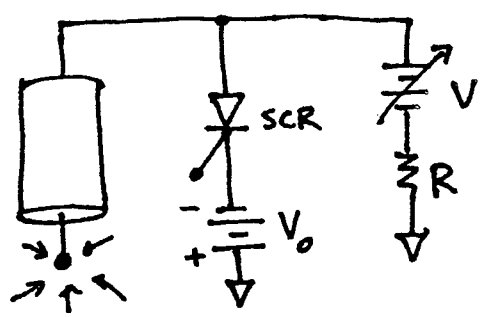

FIG. 12

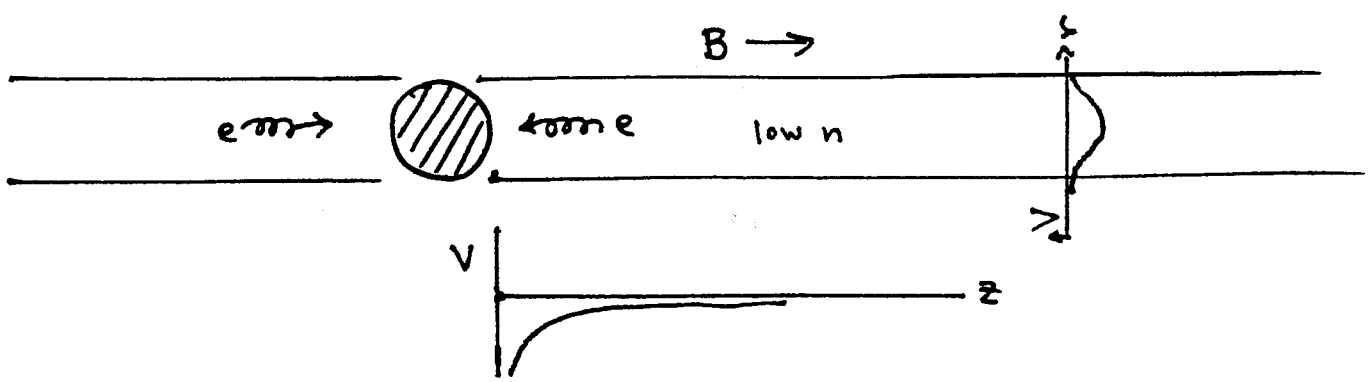

FIG. 13

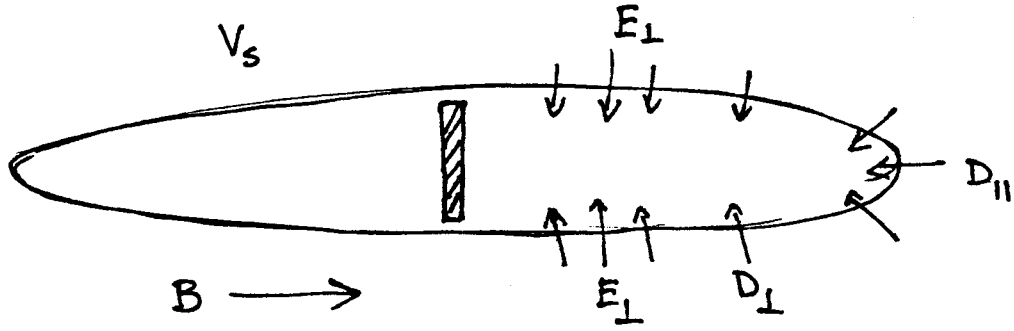

FIG. 14

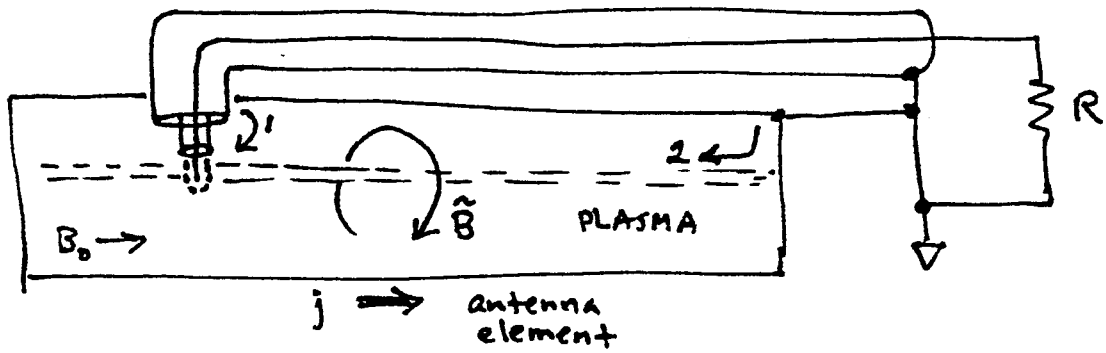

FIG. 15

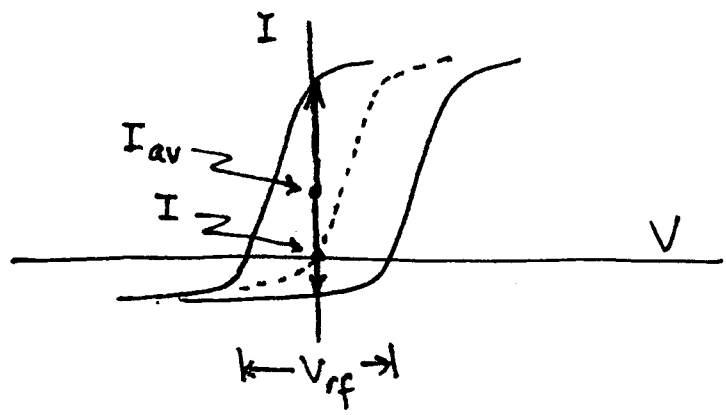

FIG. 16

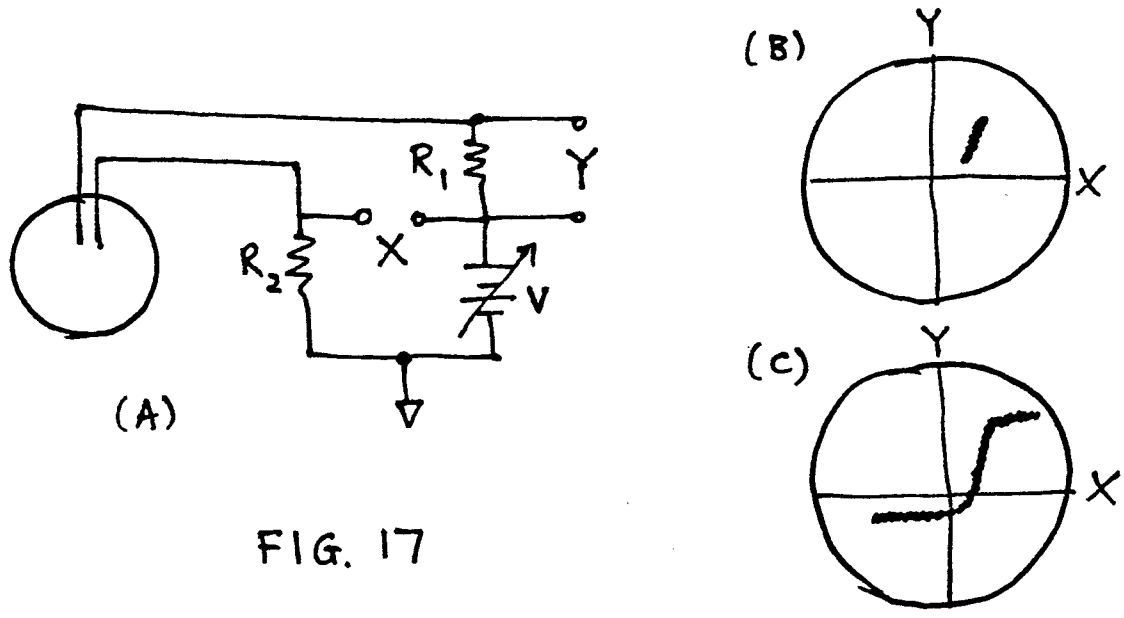

FIG. 17

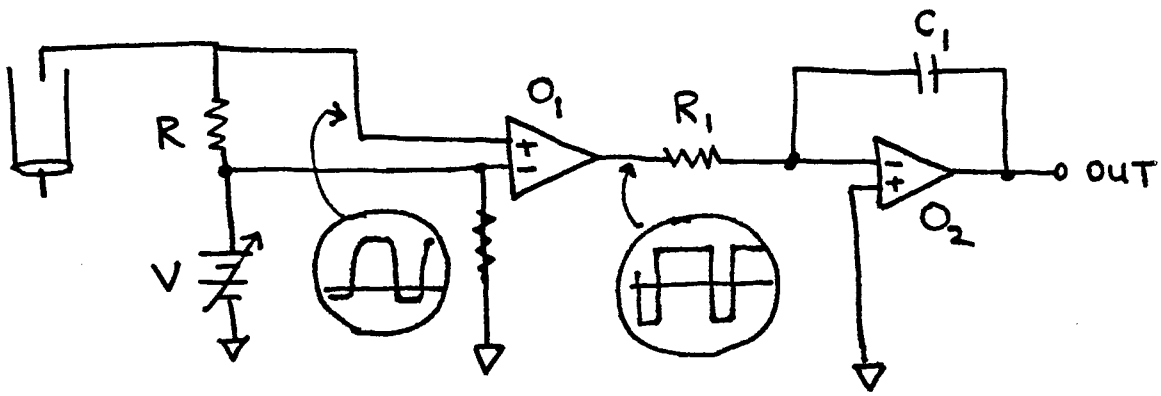

FIG. 18

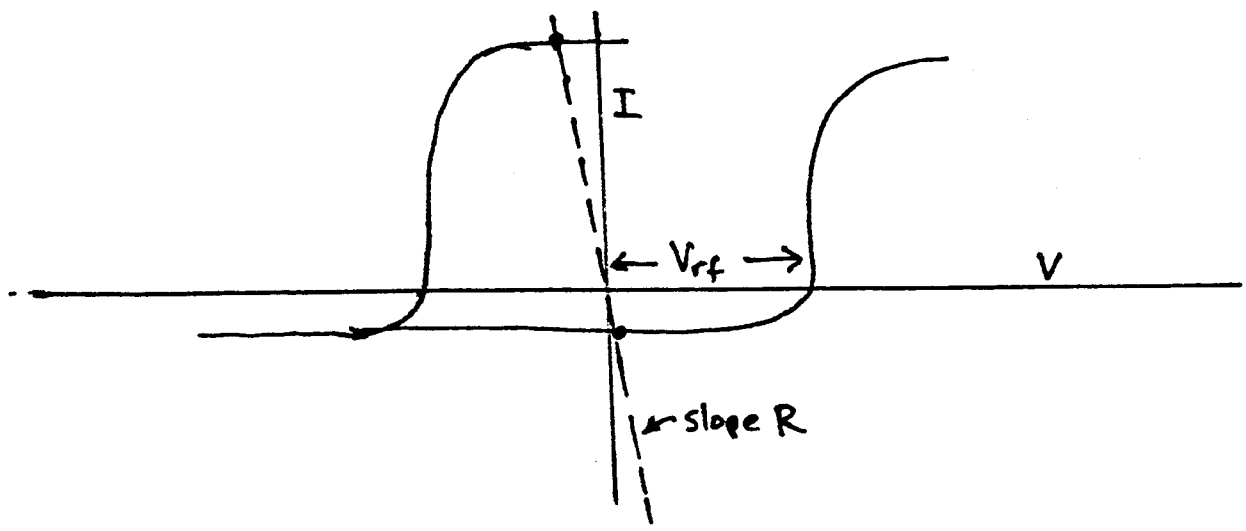

FIG. 19

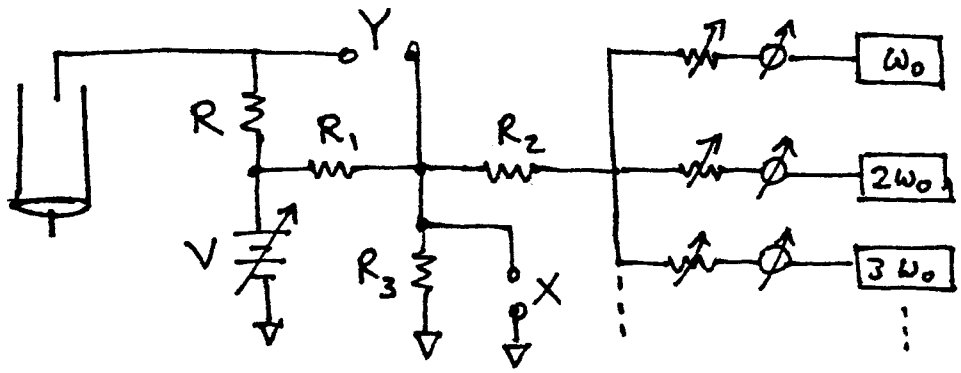

FIG. 20

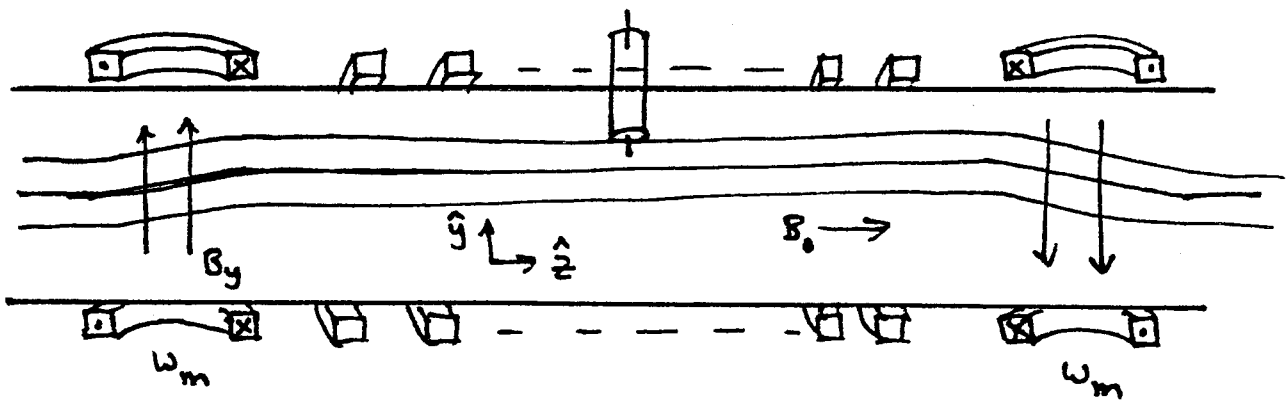

FIG. 21

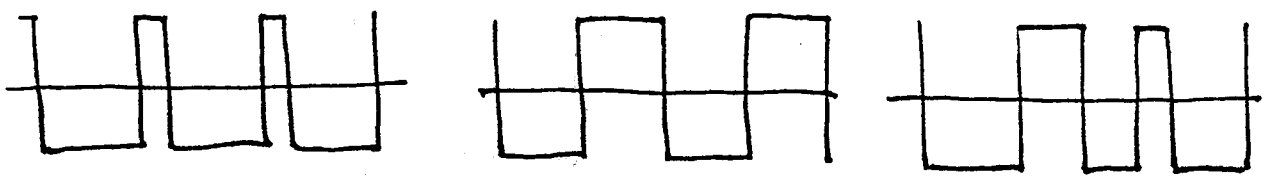

FIG. 22